

# UC Irvine

## UC Irvine Previously Published Works

### Title

A new atmospherically relevant oxidant of sulphur dioxide

### Permalink

<https://escholarship.org/uc/item/3s69m0tk>

### Journal

Nature, 488(7410)

### ISSN

0028-0836

### Authors

Mauldin III, RL  
Berndt, T  
Sipilä, M  
et al.

### Publication Date

2012-08-01

### DOI

10.1038/nature11278

### Copyright Information

This work is made available under the terms of a Creative Commons Attribution License, available at <https://creativecommons.org/licenses/by/4.0/>

Peer reviewed

# A new atmospherically relevant oxidant of sulphur dioxide

R. L. Mauldin III<sup>1,2,3</sup>, T. Berndt<sup>4</sup>, M. Sipilä<sup>1,4,5</sup>, P. Paasonen<sup>1</sup>, T. Petäjä<sup>1</sup>, S. Kim<sup>2</sup>, T. Kurtén<sup>1,6</sup>, F. Stratmann<sup>4</sup>, V.-M. Kerminen<sup>1</sup> & M. Kulmala<sup>1</sup>

**Atmospheric oxidation is a key phenomenon that connects atmospheric chemistry with globally challenging environmental issues, such as climate change<sup>1</sup>, stratospheric ozone loss<sup>2</sup>, acidification of soils and water<sup>3</sup>, and health effects of air quality<sup>4</sup>. Ozone, the hydroxyl radical and the nitrate radical are generally considered to be the dominant oxidants that initiate the removal of trace gases, including pollutants, from the atmosphere. Here we present atmospheric observations from a boreal forest region in Finland, supported by laboratory experiments and theoretical considerations, that allow us to identify another compound, probably a stabilized Criegee intermediate (a carbonyl oxide with two free-radical sites) or its derivative, which has a significant capacity to oxidize sulphur dioxide and potentially other trace gases. This compound probably enhances the reactivity of the atmosphere, particularly with regard to the production of sulphuric acid, and consequently atmospheric aerosol formation. Our findings suggest that this new atmospherically relevant oxidation route is important relative to oxidation by the hydroxyl radical, at least at moderate concentrations of that radical. We also find that the oxidation chemistry of this compound seems to be tightly linked to the presence of alkenes of biogenic origin.**

Oxidation of trace gases drives atmospheric chemistry and influences thereby both air quality and climate, and their interaction with each other and the biosphere<sup>1,5–7</sup>. The main gas-phase oxidants under consideration (so far) are the OH radical (OH<sup>\*</sup>, referred to here as OH for simplicity), O<sub>3</sub>, the nitrate radical (NO<sub>3</sub><sup>\*</sup>, referred to here as NO<sub>3</sub> for simplicity) and Cl atoms, of which OH is important only during the daytime and NO<sub>3</sub> during night time. Recently, an increasing number of investigations have focused on atmospheric reactivity, more specifically the missing reactivity<sup>8,9</sup> and sources<sup>5,10</sup> of OH and its temporal variability<sup>11</sup>, as well as missing HONO sources<sup>7</sup>. Sulphuric acid (H<sub>2</sub>SO<sub>4</sub>) is a key compound, connecting atmospheric oxidation chemistry with the formation and growth of new aerosol particles<sup>12</sup>. Until now, the general consensus has been that the rate at which sulphur dioxide (SO<sub>2</sub>) is converted to gaseous H<sub>2</sub>SO<sub>4</sub> is determined by the OH concentration. Here we show that there is another important source of gaseous H<sub>2</sub>SO<sub>4</sub> that is not directly related to OH.

Our investigation into this uncharted oxidation chemistry is based on simultaneous observations of OH and H<sub>2</sub>SO<sub>4</sub> using chemical ionization mass spectrometry<sup>13</sup> (CIMS; see Supplementary Information). When measuring OH concentrations using this technique, OH is first converted to isotopically labelled H<sub>2</sub>SO<sub>4</sub> by the addition of <sup>34</sup>SO<sub>2</sub> to the ambient sample flow; the resulting H<sub>2</sub><sup>34</sup>SO<sub>4</sub> is then measured using CIMS. There are, however, other processes which can oxidize SO<sub>2</sub> to H<sub>2</sub>SO<sub>4</sub>. To determine which fraction of the measured H<sub>2</sub><sup>34</sup>SO<sub>4</sub> originates from the reaction of atmospheric OH with <sup>34</sup>SO<sub>2</sub>, the measurement is repeated with the addition of an OH scavenger (propane) to the sample flow to suppress H<sub>2</sub><sup>34</sup>SO<sub>4</sub> formation via OH. This procedure results in a 'background' H<sub>2</sub><sup>34</sup>SO<sub>4</sub>

concentration (produced from X + SO<sub>2</sub>), termed [X] here, which is subtracted from the total H<sub>2</sub><sup>34</sup>SO<sub>4</sub> concentration to obtain the ambient OH concentration. We hypothesize that [X] represents a yet unexplored oxidant X (or sum of several such oxidants) which, similarly to OH, is capable of converting SO<sub>2</sub> to gaseous sulphuric acid in the atmosphere.

We started our investigation using field observations performed at the SMEAR II station in the Finnish boreal forest region (Supplementary Information). Figure 1a and b shows the concentration time series of [OH], [X] and [H<sub>2</sub>SO<sub>4</sub>] measured over one week during the summer of 2010. The OH concentration shows a typical diurnal cycle<sup>14</sup>, with maximum concentrations around noon and much lower ones during the night. The value of [X] does not show a clear diurnal cycle, but it typically exceeds [OH]. During several evenings and nights, we identify instances when [OH] is close to 10<sup>5</sup> molecules cm<sup>-3</sup>, [X] simultaneously exceeds 10<sup>6</sup> molecules cm<sup>-3</sup>, and [H<sub>2</sub>SO<sub>4</sub>] is remarkably high, up to about 10<sup>6</sup> molecules cm<sup>-3</sup>. This observation indicates the presence of a non-OH source for H<sub>2</sub>SO<sub>4</sub> production, and further suggests that there might be a connection between this source and the oxidant X. We calculated the H<sub>2</sub>SO<sub>4</sub> concentration resulting from the reaction of SO<sub>2</sub> with OH (green line in Fig. 1b). The difference between the H<sub>2</sub>SO<sub>4</sub> concentration measured by the CIMS and that due to the reaction of SO<sub>2</sub> with OH is our best estimate of the H<sub>2</sub>SO<sub>4</sub> concentration resulting from the non-OH source, [H<sub>2</sub>SO<sub>4</sub>]<sub>non-OH</sub>. Figure 1c shows that the value of [H<sub>2</sub>SO<sub>4</sub>]<sub>non-OH</sub> increases with increasing [X], reaching values as high as (2–3) × 10<sup>6</sup> molecules cm<sup>-3</sup> during our measurements. Sulphuric acid originating from this non-OH source may contribute up to 50% of the total H<sub>2</sub>SO<sub>4</sub> budget (Fig. 1b and Supplementary Information), demonstrating the important role of this H<sub>2</sub>SO<sub>4</sub> formation route.

The dominance of [X] over [OH] particularly during evenings and nights suggests that the compound X might be related to surface emissions and subsequent ozone chemistry taking place in the boundary layer. In order to investigate this chemistry, we carried out laboratory experiments using two systems with different flow characteristics (Supplementary Information). In these experiments, SO<sub>2</sub> was exposed to mixtures of ozone and various alkenes, and the resulting H<sub>2</sub>SO<sub>4</sub> concentration was measured with CIMS and modelled using a scheme based on known OH chemistry (Supplementary Information). Because alkene–ozone reactions are known to produce OH, the experiments were conducted both with and without an OH-scavenger (H<sub>2</sub> or CO). Figure 2a shows the measured and modelled H<sub>2</sub>SO<sub>4</sub> concentration as a function of the amount of monoterpene (limonene and α-pinene) reacted with ozone. As in the field study, we observed H<sub>2</sub>SO<sub>4</sub> that cannot be explained by the reaction of SO<sub>2</sub> with OH alone. In these experiments, the production of H<sub>2</sub>SO<sub>4</sub> from this non-OH source appeared to be more efficient for monoterpenes than for other alkenes (for example, MCH, 1-methyl-cyclohexene; see Supplementary Information). The role of the new H<sub>2</sub>SO<sub>4</sub> production chemistry

<sup>1</sup>University of Helsinki, Department of Physics, FI-00014 Helsinki, Finland. <sup>2</sup>National Center for Atmospheric Research, Boulder, Colorado 80307, USA. <sup>3</sup>Department of Atmospheric and Oceanic Sciences, University of Colorado at Boulder, Boulder, Colorado 80309, USA. <sup>4</sup>Leibniz-Institute for Tropospheric Research, 04318 Leipzig, Germany. <sup>5</sup>Helsinki Institute of Physics, FI-00014 Helsinki, Finland.

<sup>6</sup>University of Helsinki, Department of Chemistry, FI-00014 Helsinki, Finland.

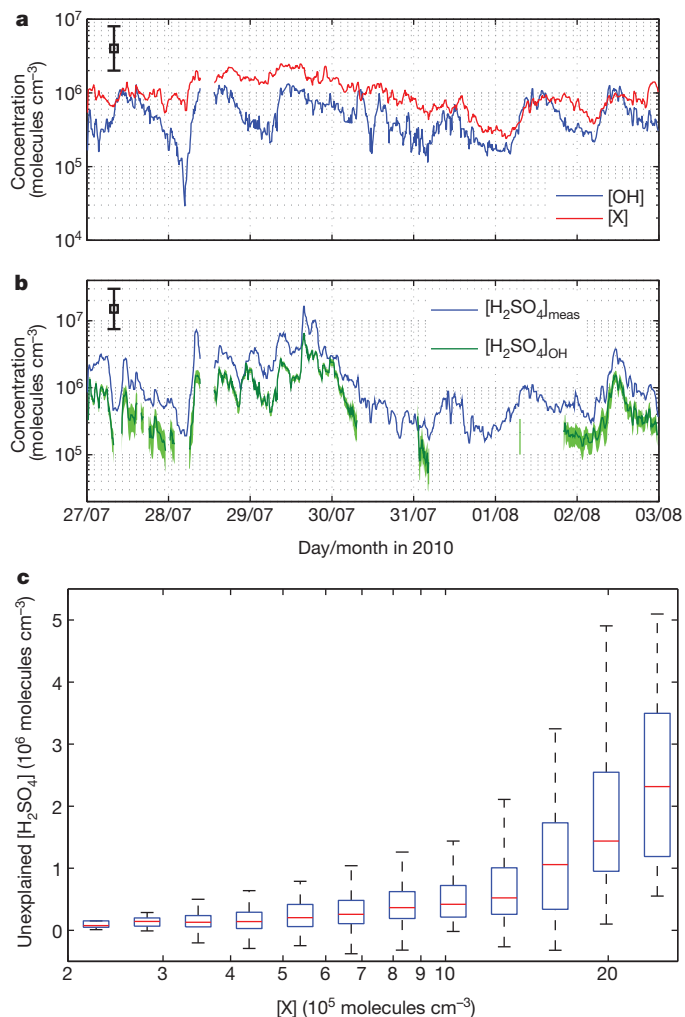


**Figure 1** | Data from a boreal forest site, obtained during summer 2010. **a**, Time series of [OH] (blue line) and of [X] (red line); **b**, time series of the  $\text{H}_2\text{SO}_4$  concentration measured by CIMS (blue line), and of the  $\text{H}_2\text{SO}_4$  concentration attributable to the reaction of OH with  $\text{SO}_2$ ,  $[\text{H}_2\text{SO}_4]_{\text{OH}}$  (green line); data were obtained from 27 July to 3 August 2010 at Hyttälä, Finland. The value of  $[\text{H}_2\text{SO}_4]_{\text{OH}}$  is determined on the basis of the measured  $\text{SO}_2$  and OH concentrations and the calculated condensation sink for gaseous  $\text{H}_2\text{SO}_4$ , ref. 30. **c**, Estimated concentration of  $\text{H}_2\text{SO}_4$  attributable to the non-OH source as a function of [X]. Red lines are median values; boxes depict 25th and 75th percentiles; black bars enclose all data excluding outliers. We now consider uncertainties in **a** and **b**. The vertical bars in the upper left corners of **a** and **b** illustrate the uncertainty range ( $\pm$  a factor of 2) in the measured values of  $[\text{H}_2\text{SO}_4]$  and [OH], as well as in measured [X] under the assumption that X is fully converted to  $[\text{H}_2^{34}\text{SO}_4]$ . These are absolute uncertainties, based on the stated uncertainties of the values used in the calculation (such as CIMS calibration lamp intensity, water photolysis reaction rate coefficient and OH losses). The statistical uncertainties are less important in comparison with these uncertainties. The shaded green area in **b** depicts the range of additional uncertainty in calculated  $[\text{H}_2\text{SO}_4]_{\text{OH}}$  obtained by taking into account the uncertainties in the measured values of the  $\text{SO}_2$  concentration ( $\pm 0.05$  p.p.b.) and condensation sink. The upper limit of each error estimate was calculated by assuming that the  $\text{SO}_2$  concentration was 0.05 p.p.b. larger than the measured value and that the condensation sink was at its minimum value at the measured relative humidity. The minimum value of the condensation sink, CS, was obtained by assuming that there were no super-micrometre particles and that the hygroscopicity of the sub-micrometre particles was at its minimum. Consequently, the lower limit of each error estimate was calculated by assuming that the  $\text{SO}_2$  concentration was 0.05 p.p.b. lower than the measured value, and that the condensation sink was at its maximum value at the measured relative humidity. The maximum value of CS was obtained by assuming that the super-micrometre particles contributed 5% to total CS, and that the hygroscopicity of the sub-micrometre particles was at its maximum (see Supplementary Information and references therein).

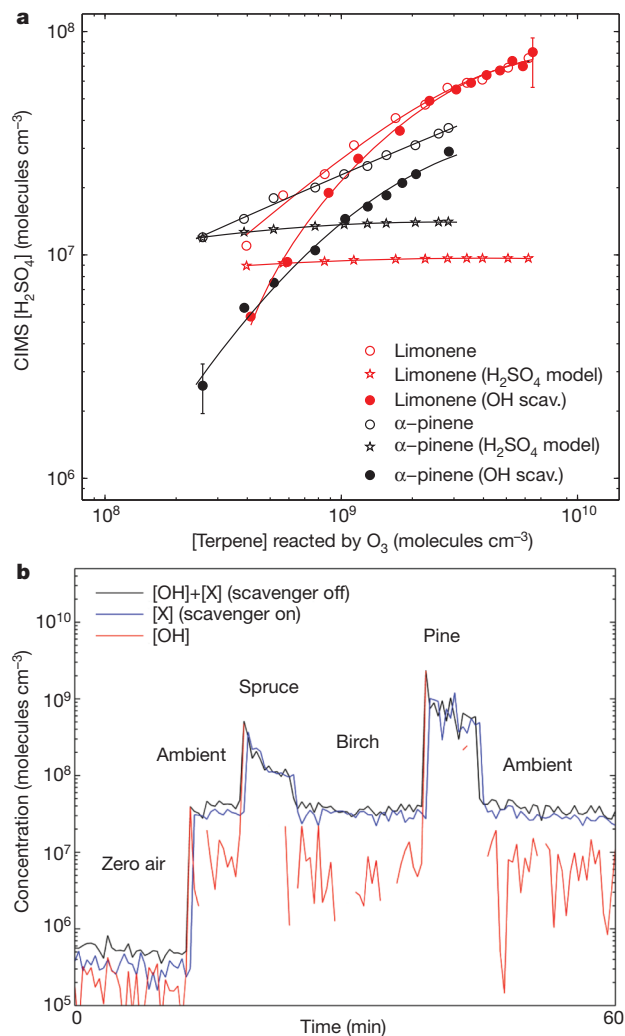


**Figure 2** | Plots showing that alkenes emitted by vegetation are possibly the source of oxidant X. Measured  $\text{H}_2\text{SO}_4$  concentrations as a function of reacted terpene concentration ( $\alpha$ -pinene or limonene) in the presence and absence of an OH scavenger ( $\text{H}_2$ ) as a result of IFT-LFT laboratory experiments. Data were obtained using constant  $\text{O}_3$  and  $\text{SO}_2$  concentrations ( $\text{O}_3$ , 24.7 p.p.b.v.;  $\text{SO}_2$ , 14.6 p.p.b.v.), and  $[\text{H}_2]$  was  $2.4 \times 10^{17}$  molecules  $\text{cm}^{-3}$ . Modelling results (including only  $\text{H}_2\text{SO}_4$  formation via OH +  $\text{SO}_2$ ) are shown for runs in the absence of the OH scavenger; compare the reaction scheme shown in Supplementary Information. The results from limonene when compared with those from  $\alpha$ -pinene clearly show that the former is more efficient at producing the additional  $\text{H}_2\text{SO}_4$ . Error bars are  $\pm 35\%$  and indicate the uncertainty in  $\text{H}_2\text{SO}_4$  measurements; they represent an absolute uncertainty resulting from a propagation of uncertainties in the CIMS calibration lamp intensity, water photolysis reaction rate coefficient and OH losses (see details in Supplementary information). **b**, Pine and spruce are potentially major species emitting precursors of X. Here data series show the measured concentration of all oxidants (OH and X) capable of oxidizing  $\text{SO}_2$  in absence of an OH scavenger, the measured concentration of X in the presence of an OH scavenger, as well as the difference between the two, which corresponds to the concentration of OH. Data were obtained in Hyttälä, a boreal forest site in late summer (5 September 2011). Zero air measurements indicate the level of instrumental background. Measurements were performed by placing the branches from different tree varieties in the direct vicinity of the instrument's inlet, one species at the time. VOCs emitted by the branches react with ambient  $\text{O}_3$ , subsequently producing OH and sCI. As [OH] is calculated from the difference of measured  $[\text{OH}] + [\text{X}]$  and [X], [OH] cannot be accurately determined during high [X] (pine and spruce). Both spruce and pine yielded enormous increases in signal, while birch had no observable effect (see Supplementary Information for a complete figure). Cutting of branches results in enlarged emissions of monoterpenes from trees with large storage pools, such as spruce (*Picea abies*) and pine (*Pinus sylvestris*)<sup>15</sup>.

becomes dominant at high monoterpene concentrations, as shown by the convergence of the data series taken in the absence and in the presence of the OH scavenger.

Monoterpenes, including limonene and  $\alpha$ -pinene used in our experiments, are emitted effectively by trees, and these compounds are abundantly present at our field measurement site during the summertime<sup>15,16</sup>. To confirm vegetation as a source of the alkenes responsible for X formation in the boreal forest environment, we performed an additional experiment where branches of different trees were cut and placed in the immediate vicinity of the CIMS inlet (Fig. 2b, see also Supplementary Information). The production of OH from ozonolysis of branch emissions during this experiment was minor in comparison to production of X. This experiment indisputably substantiates our conclusion, demonstrating the role of trees in producing compound X and, consequently, affecting gaseous sulphuric acid production.

The field and laboratory measurements presented above give strong evidence of the existence of a previously unknown oxidant X, but do not reveal its identity. Experiments<sup>17,18</sup> and quantum chemical calculations<sup>19,20</sup> have demonstrated that the reactions of SO<sub>2</sub> with the most common non-OH oxidants (O<sub>3</sub> and NO<sub>3</sub>) and with peroxy radicals (HO<sub>2</sub>, H<sub>3</sub>COO and larger analogues) are extremely slow. Stabilized Criegee intermediates (sCIs), formed in the ozonolysis of all alkenes, are known to oxidize SO<sub>2</sub> (ref. 21) but the rate constant of the SO<sub>2</sub> + sCI reaction has been assumed to be fairly low, of the order of 10<sup>-15</sup> cm<sup>3</sup> s<sup>-1</sup> (ref. 22). However, recent theoretical quantum mechanical studies<sup>20,23</sup>, as well as laboratory experiments<sup>24</sup>, have found the SO<sub>2</sub> + sCI reaction to be significantly faster than previously thought. Another property that influences the oxidation capacity of sCIs is their lifetime against unimolecular decomposition reactions. The sCIs formed in ozonolysis of larger alkenes, such as monoterpenes, may have longer lifetimes than those formed from lower-molecular-weight alkenes. We note here that besides sCIs, other ozonolysis intermediates might also be responsible for the observed additional oxidation of SO<sub>2</sub> (refs 25, 26). Figure 3 summarizes schematically this new mechanism of atmospheric oxidation chemistry.

We finalize our analysis by investigating whether the proposed chemistry is consistent with field observations. For this purpose, we estimated the reaction rate between sCI and SO<sub>2</sub> from the laboratory measurement data presented in Fig. 2a (see Supplementary Information for theoretical considerations and assumptions made in deriving the reaction rate). The resulting rate coefficient was about 6 × 10<sup>-13</sup>

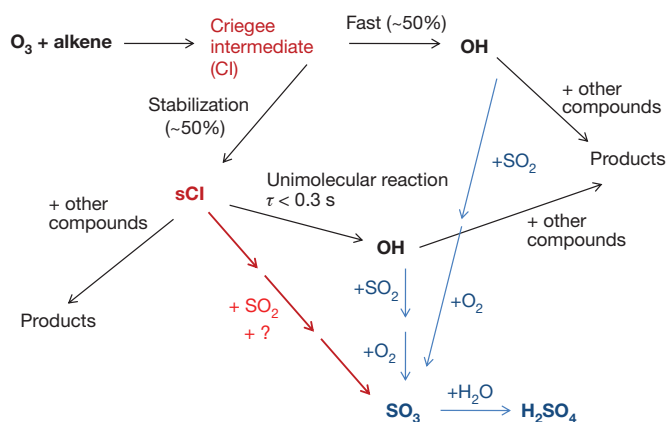


**Figure 3 | Proposed mechanism for the formation of oxidant X.** Of the Criegee intermediates (CI) formed during ozonolysis, ~50% decompose to produce OH on a subsecond timescale while the other 50% are stabilized, producing stabilized Criegee radicals, sCI. These sCI can then decompose over a much longer lifetime,  $\tau$ . Our observations suggest that sCI, or non-OH derivatives of sCI, can also oxidize at least SO<sub>2</sub> (red arrows), thus altering the known view of oxidation chemistry in the atmosphere. Typical OH chemistry is depicted in blue.

cm<sup>3</sup> s<sup>-1</sup> for  $\alpha$ -pinene + sCI and about 8 × 10<sup>-13</sup> cm<sup>3</sup> s<sup>-1</sup> for limonene + sCI. In Fig. 4a and b we have calculated the H<sub>2</sub>SO<sub>4</sub> concentration originating from the two SO<sub>2</sub> oxidation pathways, OH and non-OH, during the field measurement period reported in Fig. 1. The comparison of the calculated values of [H<sub>2</sub>SO<sub>4</sub>] with the measured ones shows that in addition to explaining the large missing H<sub>2</sub>SO<sub>4</sub> source

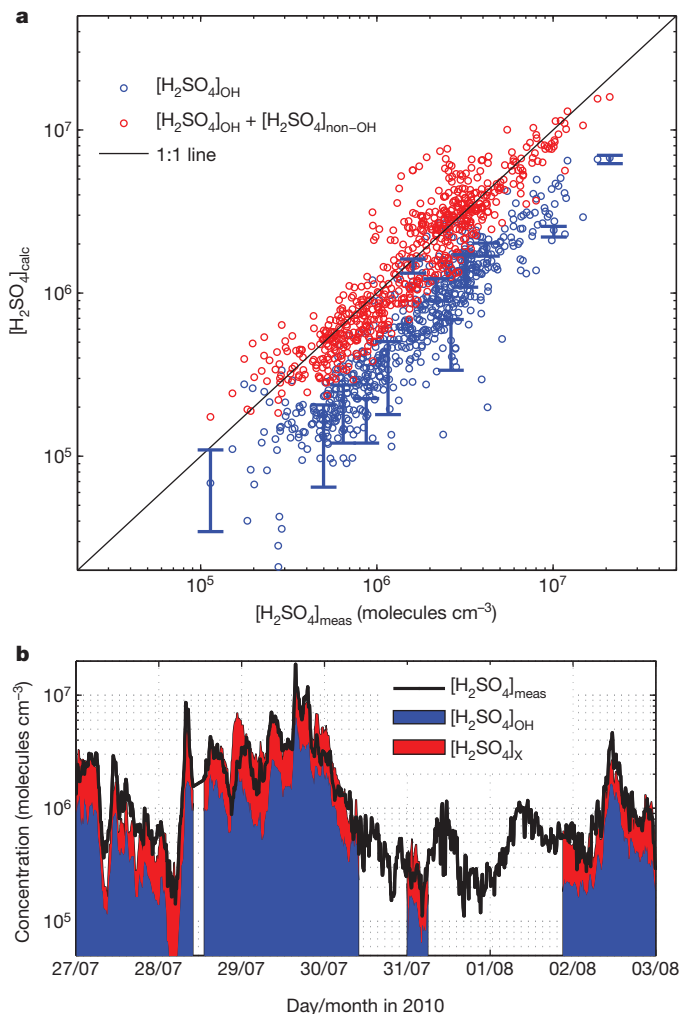


**Figure 4 | H<sub>2</sub>SO<sub>4</sub> produced from X + SO<sub>2</sub> can explain the difference between the Hyytiälä 2010 H<sub>2</sub>SO<sub>4</sub> measurements and calculated values using only OH + SO<sub>2</sub>.** **a**, Calculated sulphuric acid concentration as a function of the measured concentration. Blue circles represent the concentration calculated for SO<sub>2</sub> oxidation solely via OH, whereas the red circles correspond to the concentration calculated for SO<sub>2</sub> oxidation by both OH and X. The reaction rate coefficient for OH oxidation was taken from literature<sup>30</sup> and that for X oxidation determined from the laboratory experiments (Fig. 2) described in the text and Supplementary Information. The error in [H<sub>2</sub>SO<sub>4</sub>]<sub>OH</sub> is estimated as described for the shaded green area shown in Fig. 1, and for clarity is plotted for a few data points only. This error cannot explain the observed systematic difference between [H<sub>2</sub>SO<sub>4</sub>]<sub>OH</sub> and [H<sub>2</sub>SO<sub>4</sub>]<sub>meas</sub> (the average ratio between these quantities being 0.41). The error in [H<sub>2</sub>SO<sub>4</sub>]<sub>non-OH</sub> cannot be accurately quantified and therefore no error estimate for the red data points has been given. The errors resulting from uncertainties in measured OH or H<sub>2</sub>SO<sub>4</sub> concentrations do not affect the position of blue or red points with respect to the one-to-one line. Correlation coefficients (log-log scale) for the two data series are R<sup>2</sup> = 0.81 and R<sup>2</sup> = 0.85 for OH only and OH with X, respectively. **b**, The same time series as presented in Fig. 1a, now showing, in addition to [H<sub>2</sub>SO<sub>4</sub>]<sub>meas</sub> (black line) and calculated from OH reaction (blue area), the concentration calculated from the X reaction as in **a** (red area). Between 30 July and 2 August, the SO<sub>2</sub> concentration was mostly below the detection limit during which time the calculated concentration is not depicted. The error bars, not shown for clarity, are essentially the same as in Fig. 1a.

during some evenings and nights, addition of the new SO<sub>2</sub> oxidant significantly improves the overall agreement between measured and calculated H<sub>2</sub>SO<sub>4</sub> concentrations.

The chemistry investigated here is tightly connected with the presence of biogenic volatile organic compounds (BVOCs), and thereby with forest emissions. Covering vast areas of the Earth's surface, forests play an important role in global cycles of carbon, water and energy<sup>6</sup>. BVOCs emitted by forests dominate the global secondary organic aerosol loading<sup>27</sup>, and contribute significantly to the global budget of cloud condensation nuclei<sup>28</sup>. Our findings add to the already substantial significance of forests in the Earth system by introducing a previously unknown oxidant, probably an sCl, capable of oxidizing at least SO<sub>2</sub> and possibly also other atmospheric trace gases relevant to atmospheric chemistry. Because gaseous sulphuric acid is formed in this process, the new chemistry is likely to affect the formation of new atmospheric particles, the production of secondary cloud condensation nuclei and ultimately climate. Our findings demonstrate a new connection between anthropogenic activities (SO<sub>2</sub> emissions), natural ecosystems (BVOC emissions and secondary organic aerosol formation) and climate (from cloud properties to radiative forcing). This connection is likely to change in the future as a result of changing SO<sub>2</sub> and BVOC emissions due to air quality regulations and warming climate<sup>29</sup>. More detailed experimental and theoretical investigations are clearly needed to find out the importance of the new oxidant in atmospheric chemistry and climate at present and under future conditions.

## METHODS SUMMARY

The results of the laboratory experiments described here were obtained from two different experimental systems. Both systems used the flow tube (that is, continuous flow) technique, where gases are added to a continuous stream and allowed to react for a known period of time. Sulphuric acid was then measured at the exit of the flow tube using nitrate-ion-based chemical ionization mass spectrometry (CIMS). One experimental apparatus (referred to as IfT-LFT) was located at the Leibniz-Institute for Tropospheric Research in Leipzig, Germany, and the other at the National Center for Atmospheric Research (NCAR) in Boulder, Colorado. The two systems differ from each other in their geometries, residence times and the method by which the reagent gases are introduced. The CIMS instrument was also used in the field measurements performed at the SMEAR II station located in a Finnish boreal forest for the detection of H<sub>2</sub>SO<sub>4</sub>, OH and X. A more detailed description of the methods is given in Supplementary Information.

**Full Methods** and any associated references are available in the online version of the paper.

Received 23 November 2011; accepted 10 May 2012.

- Liao, H. *et al.* Effect of chemistry-aerosol-climate coupling on predictions of future climate and future levels of tropospheric ozone and aerosols. *J. Geophys. Res.* **114**, D10306, <http://dx.doi.org/10.1029/2008JD010984> (2009).
- Rowland, F. S. Stratospheric ozone depletion. *Phil. Trans. R. Soc. Lond. B* **361**, 769–790 (2006).
- Likens, G. E., Bormann, F. H. & Johnson, N. M. Acid rain. *Environment* **14**, 33–40 (1974).
- Fenger, J. Air pollution in the last 50 years — from local to global. *Atmos. Environ.* **43**, 13–22 (2009).
- Lelieveld, J. *et al.* Atmospheric oxidation capacity sustained by a tropical forest. *Nature* **452**, 737–740 (2008).
- Arneth, A. *et al.* Terrestrial biogeochemical feedbacks in the climate system. *Nature Geosci.* **3**, 525–532 (2010).
- Su, H. *et al.* Soil nitrite as a source of atmospheric HONO and OH radicals. *Science* **333**, 1616–1618 (2011).
- Di Carlo, P. *et al.* Missing OH reactivity in a forest: evidence for unknown reactive biogenic VOCs. *Science* **304**, 722–725 (2004).
- Lou, S. *et al.* Atmospheric OH reactivities in the Pearl River Delta – China in summer 2006: measurements and model results. *Atmos. Chem. Phys.* **10**, 11243–11260 (2010).

- Hofzumahaus, A. *et al.* Amplified trace gas removal in the troposphere. *Science* **324**, 1702–1704 (2009).
- Montzka, S. A. *et al.* Small interannual variability of global atmospheric hydroxyl. *Science* **331**, 67–70 (2011).
- Sipilä, M. *et al.* The role of sulfuric acid in atmospheric nucleation. *Science* **327**, 1243–1246 (2010).
- Eisele, F. L. & Tanner, D. J. Ion-assisted tropospheric OH measurements. *J. Geophys. Res.* **96**, 9295–9308 (1991).
- Petäjä, T. *et al.* Sulfuric acid and OH concentrations in a boreal forest site. *Atmos. Chem. Phys.* **9**, 7435–7448 (2009).
- Hakola, H. Seasonal variation of VOC concentrations above a boreal coniferous forest. *Atmos. Environ.* **37**, 1623–1634 (2003).
- Lappalainen, H. K. *et al.* Day-time concentrations of biogenic volatile organic compounds in a boreal forest canopy and their relation to environmental and biological factors. *Atmos. Chem. Phys.* **9**, 5447–5459 (2009).
- Cocks, A. T., Fernando, R. P. & Fletcher, I. S. The gas-phase reaction of the methylperoxy radical with sulphur dioxide. *Atmos. Environ.* **20**, 2359–2366 (1986).
- Xie, Z. D. Formation mechanism of condensation nuclei in nighttime atmosphere and the kinetics of the SO<sub>2</sub>-O<sub>3</sub>-NO<sub>2</sub> system. *J. Phys. Chem.* **96**, 1543–1547 (1992).
- Kurtén, T., Lane, J. R., Jørgensen, S. & Kjaergaard, H. Nitrate radical addition-elimination reactions of atmospherically relevant sulfur-containing molecules. *Phys. Chem. Chem. Phys.* **12**, 12833–12839 (2010).
- Kurtén, T., Lane, J. R., Jørgensen, S. & Kjaergaard, H. A. Computational study of the oxidation of SO<sub>2</sub> to SO<sub>3</sub> by gas-phase organic oxidant. *J. Phys. Chem. A* **115**, 8669–8681 (2011).
- Hatakeyama, S., Kobayashi, H., Lin, Z.-Y., Tagaki, H. & Akimoto, H. Mechanism for the reaction of H<sub>2</sub>COO with SO<sub>2</sub>. *J. Phys. Chem.* **90**, 4131–4135 (1986).
- Johnson, D., Lewin, A. G. & Marston, G. The effect of Criegee-intermediate scavengers on the OH yield from the reaction of ozone with 2-methylbut-2-ene. *J. Phys. Chem. A* **105**, 2933–2935 (2001).
- Jiang, L., Xu, Y. & Ding, A. J. Reaction of stabilized Criegee intermediates from ozonolysis of limonene with sulfur dioxide: ab initio and DFT study. *J. Phys. Chem. A* **114**, 12452–1246 (2010).
- Welz, O. *et al.* Direct kinetic measurements of Criegee intermediate (CH<sub>2</sub>OO) formed by reaction of CH<sub>2</sub>I with O<sub>2</sub>. *Science* **335**, 204–207 (2012).
- Cox, R. A. & Penkett, S. A. Oxidation of atmospheric SO<sub>2</sub> by products of the ozone-olefin reaction. *Nature* **230**, 321–322 (1971).
- Drozd, G. T., Kroll, J. & Donahue, N. M. 2,2-Dimethyl-2-butene (TME) ozonolysis: pressure dependence of stabilized Criegee intermediates and evidence of stabilized vinyl hydroperoxides. *J. Phys. Chem. A* **115**, 161–166 (2011).
- Heald, C. L. *et al.* Predicted change in global secondary organic aerosol concentrations in response to future climate, emissions, and land use change. *J. Geophys. Res.* **113**, D05211, <http://dx.doi.org/10.1029/2007JD009092> (2008).
- Spracklen, D. V. *et al.* Contribution of particle formation to global cloud condensation nuclei concentrations. *Geophys. Res. Lett.* **35**, L06808, <http://dx.doi.org/10.1029/2007GL033038> (2008).
- Arneth, A., Unger, N., Kulmala, M. & Andreae, M. O. Clean the air, heat the planet? *Science* **326**, 672–673 (2009).
- DeMore, W. *et al.* *Chemical Kinetics and Photochemical Data for Use in Stratospheric Modeling. Evaluation 12*. JPL Publication 97-4 (Jet Propulsion Laboratory, 1997).

**Supplementary Information** is linked to the online version of the paper at [www.nature.com/nature](http://www.nature.com/nature).

**Acknowledgements** We thank K. Pielok and A. Rohmer for technical assistance. This work was partially funded by the European Commission Sixth Framework programme project EUCAARI, contract no. 036833-2 (EUCAARI), the Academy of Finland (251427, 139656, Finnish centre of excellence 141135), the European Research Council (ATMNUCLE), the Kone Foundation, the Väisälä Foundation, the Maj and Tor Nessling Foundation (2010212), the Otto Malm Foundation and the US National Science Foundation.

**Author Contributions** R.L.M., T.B. and M.S. designed the experiments. R.L.M., T.B., M.S. and S.K. performed the laboratory experiments, R.L.M., T.P. and M.S. conducted the field measurements, T.B., T.K., and P.P. performed the model and theoretical calculations, and R.L.M., T.B., M.S. and P.P. analysed the data. All authors (R.L.M., T.B., M.S., P.P., T.P., S.K., T.K., F.S., V.-M.K., and M.K.) contributed to the interpretation and to manuscript preparation.

**Author Information** Reprints and permissions information is available at [www.nature.com/reprints](http://www.nature.com/reprints). The authors declare no competing financial interests. Readers are welcome to comment on the online version of this article at [www.nature.com/nature](http://www.nature.com/nature). Correspondence and requests for materials should be addressed to R.L.M. ([roy.mauldin@helsinki.fi](mailto:roy.mauldin@helsinki.fi)).

## METHODS

**CIMS measurements.** Measurements of OH and H<sub>2</sub>SO<sub>4</sub> were performed using the Chemical Ionization Mass Spectrometer (CIMS) technique. The technique has been described elsewhere<sup>13,31,32</sup> therefore only details relevant to the present work will be discussed here. Briefly, sample air is drawn through the 1.9 cm stainless steel inlet, and a small amount ( $\sim 10^{14}$  molecules cm<sup>-3</sup>) of isotopically labelled <sup>34</sup>SO<sub>2</sub> is added through a pair of 0.011 cm i.d. transversely opposed injectors located near the front opening. The OH is then converted into H<sub>2</sub><sup>34</sup>SO<sub>4</sub> via the following reaction sequence:



Isotopically labelled SO<sub>2</sub> is used to discriminate between H<sub>2</sub>SO<sub>4</sub> derived from OH and ambient H<sub>2</sub>SO<sub>4</sub>. To prevent cycling of HO<sub>2</sub> and RO<sub>2</sub> back into OH, propane is added on a continuous basis through a second pair of injectors located  $\sim 5$  cm downstream of the first pair, after the ambient OH initially present has been converted into H<sub>2</sub>SO<sub>4</sub>. Propane is added through these injectors at sufficient concentrations to remove more than 99% of the OH which has been cycled back from HO<sub>2</sub> or RO<sub>2</sub> via reactions with NO or O<sub>3</sub>. To account for other unknown processes which can convert SO<sub>2</sub> into H<sub>2</sub>SO<sub>4</sub> an 'OH background' is performed, in which propane is added along with the <sup>34</sup>SO<sub>2</sub> through the front injectors at a concentration sufficient to remove >98% of the OH present. These OH background values are used in this work to describe the measurement of X. More details concerning the injectors and the sampling port chemistry are described elsewhere<sup>31</sup>. Once formed, the H<sub>2</sub><sup>34</sup>SO<sub>4</sub> is measured in the same manner as H<sub>2</sub>SO<sub>4</sub> via chemical ionization.

**IFT-LFT.** Experiments were carried out in the atmospheric pressure flow-tube IfT-LFT (i.d. 8 cm; length 505 cm) at 293  $\pm$  0.5 K (ref. 33). The flow tube consists of a first section (56 cm) that includes the inlet system for gas input (air premixed with SO<sub>2</sub> from a calibration gas mixture (1 p.p.m.v. or 10 p.p.m.v. SO<sub>2</sub> in N<sub>2</sub> (Messer)), O<sub>3</sub> from an ozone generator outside the flow tube (UVP OG-2), the OH scavenger H<sub>2</sub> and the olefin premixed from a metering device). At the end of the tube, all sampling outlets are attached. O<sub>3</sub> and SO<sub>2</sub> concentrations were measured by means of gas monitors (Thermo Environmental Instruments: 49C and 43C) or by long-path ultraviolet absorption spectroscopy (Perkin-Elmer: Lambda 800) using a gas cell with a White-mirror optics adjusted at a path-length of 512 cm. The organics were followed by proton transfer reaction-mass spectrometry (PTR-MS) or by on-line gas chromatography-flame ionization detection (GC-FID) connected via a cryo-enrichment device. Sulphuric acid in the IfT-LFT was measured with a chemical ionization mass spectrometer, CIMS, in the same way as described for the NCAR experiments. The flow was set at 15 l min<sup>-1</sup> (STP) resulting in a residence time of about 95 s.

H<sub>2</sub> (99.999%, Messer) was directly added to the carrier gas flow. As the carrier gas we used high-purity synthetic air (99.9999999%, Linde and further purification with GateKeeper CE-500KF-O-4R, Aeronex). All gas flows were set by means of calibrated gas flow controllers (MKS 1259/1179) and the pressure in the tube was measured using a capacitive manometer (Baratron).

**NCAR.** The reaction system consists of a glass flow tube with a movable stainless steel injector. A stream of hydrocarbon-free air (also called 'zero air' below)

containing SO<sub>2</sub> and the alkene being studied is added to the glass flow tube. Ozone is produced inside the stainless steel injector by passing a flow of O<sub>2</sub> over a mercury Pen-Ray lamp located inside the injector. The ozone is then introduced into the main flow at the end of the injector. The gases then can react as the flow proceeds towards the exit of the tube, where the flow is sampled. The reaction time can be varied by either adjusting the amount of the main flow, or by changing the position of the end of the injector.

The flow tube consists of a 71-cm-long Pyrex tube connected to a 20.3-cm-long Pyrex Y. Both pieces have 3.38 cm i.d. and are connected via no. 40 O-ring joints sealed with a silicone O-ring. The Pyrex Y allows access of the movable injector into the flow tube as well as providing a means to introduce the main flow. The injector consisted of a thin walled 100-cm-long, 1.27-cm-i.d. stainless steel tube with one end sealed and 24 0.2-mm holes drilled radially 0.5 cm from the sealed end. Inside the injector is a mercury Pen-Ray lamp. Ozone was produced by passing a flow of O<sub>2</sub> over the lamp. The lamp was situated such that the end of the lamp is  $\sim 5$  cm from the sealed end to prevent radiation from the lamp photolysing the main flow. The injector was inserted into the main glass flow tube by means of a no. 40 O-ring joint reduced to a 1.9-cm o.d. tube, and sealed via a Swagelok fitting modified to use silicone O-rings.

The zero air used in this system was produced by filtering ambient air via a zero air generator (Adco). The UHP (ultra-high purity) oxygen was provided by General Air and had a stated purity of 99.9999%. The SO<sub>2</sub> used was a 0.5% mixture of SO<sub>2</sub> in UHP N<sub>2</sub> and was provided by Scott Speciality Gases. Alkene mixtures were made 'in house' at NCAR, and their concentrations determined via gas chromatography. All flows into the flow tube were controlled by means of mass flow controllers (MKS).

The flow was sampled at the exit of the flow tube by a CIMS<sup>13,14</sup> (Chemical Ionization Mass Spectrometer) measuring H<sub>2</sub>SO<sub>4</sub>, a PTR-MS measuring various hydrocarbon products, and an O<sub>3</sub> analyser (2B Technologies).

**Field measurements.** Field measurements were conducted at the SMEAR II field station in Finnish boreal forest<sup>34</sup>. The station (61° 51' N, 24° 17' E) is situated in southern Finland about 60 km northeast of the city of Tampere. The nearest village with some industrial activity is approximately 10 km away, and the nearest buildings are by a small lake 500 m away from the measurement station. The station is surrounded by a coniferous Scots pine dominated forest. Other major species include spruce and birch. All field measurements discussed in this Letter were done in a container located in a small open area surrounded by the forest. The SMEAR II station is equipped with extensive meteorological and gas and aerosol instrumentation.

The calculated concentration of sulphuric acid resulting from the reaction of SO<sub>2</sub> with either OH or X was obtained by assuming a steady state between the sulphuric acid production and its loss by condensation onto pre-existing aerosol particles. Detailed descriptions of calculations are given in Supplementary Information

- Tanner, D. J., Jefferson, A. & Eisele, F. L. Selected ion chemical ionization mass spectrometric measurement of OH. *J. Geophys. Res.* **102**, 6415–6425 (1997).
- Mauldin, R. L. III *et al.* OH measurements during ACE-1: observations and model comparisons. *J. Geophys. Res.* **103**, 16713–16729 (1998).
- Berndt, T. *et al.* Laboratory study on new particle formation from the reaction OH + SO<sub>2</sub>: influence of experimental conditions, H<sub>2</sub>O vapour, NH<sub>3</sub> and the amine tert-butylamine on the overall process. *Atmos. Chem. Phys.* **10**, 7101–7116 (2010).
- Hari, P. & Kulmala, M. Station for measuring ecosystem atmosphere relations (SMEAR II). *Boreal Environ. Res.* **10**, 315–322 (2005).